Progress In Electromagnetics Research C, Vol. 27, 55–68, 2012

COMPACT DUAL BAND 1.8/3.3 GHz PLANAR MONOPOLE ANTENNAS USING TUNING MECHANISMS FOR GSM/WIMAX

C.-L. Tsai and C.-L. Yang*

Department of Electrical Engineering, National Cheng Kung University, No. 1, University Road, Tainan 70101, Taiwan

Abstract—This study is designed mainly for dual band antennas of GSM/WiMAX operation in a wireless mobile communication device. This study proposes a matching technology for single path resonance in a basic monopole antenna running in dual-mode [1] and extends to a wide tuning range. The tuning of each frequency band is complicated under the constraint of the common path of dual-mode due to mutual interaction. This study proposes a refined process and new type of antennas for excellent dual-frequency matching. The incorporation of such a matching mechanism into a tuning monopole antenna enables the flexible operation bands. Moreover, the ground plane size can be shrunk to a reasonable size, and the details will be discussed in Section 6. As a result, antennas can achieve a tuning ratio of 1.6 (from 1825 to 2943 MHz) at low frequency band. The total area of such a compact antenna including its ground can be effectively reduced to $0.018\lambda_0^2$.

1. INTRODUCTION

As the wireless telecommunication technologies become more and more mature, it is no longer a dream to access Internet wireless anywhere. The most common methods to access wireless Internet are using GSM, WLAN, and WiMAX systems. In March of 2011, IEEE approved the 802.16 m as an IMT-Advanced technology standard [2, 3]. Consequently, the applications of the WiMAX system using this new MIMO technology substantially increase the transmission data rate. This may make WiMAX technologies a potential mainstream for

Received 25 October 2011, Accepted 23 January 2012, Scheduled 29 January 2012
* Corresponding author: Chin-Lung Yang (cyang@mail.ncku.edu.tw).

accessing wireless Internet. In the present, the mobile devices are capable of accessing Internet wireless, and external universal serial bus (USB) may also support multiple bands and protocols.

Over the past five years, many WiMAX antennas for mobile devices WiMAX support WLAN bands at the same time. Studying on these literature helps us understand the antenna design for dual and multiple bands, such as [4–6] incorporating ultra-wide band (UWB) into antenna design structure. Although such designs can gain a considerably wide impedance bandwidth, they also receive a lot of noise in common operating frequencies. Other studies [7, 8] have also mentioned loop antenna and dipole antenna design structures. The dipole antennas and loop antennas could radiate omni-directional patterns which are suitable to apply to the wireless mobile communication. However, the total volume size of the combined dipole and loop antennas is larger than the monopole antenna of a $^1/_4$ wavelength. It is noteworthy that previous studies [9, 10] have discussed simple antenna design with a main electric current path creating two dual-band modes. Unlike multiple current path antennas, this design demonstrates an interference problem.

Considering the antenna design for USB in [11, 12], these studies follow the design of WLAN/WiMAX band. Recently, many vendors have developed GSM modems in USB devices. By these light and convenient terminal devices, it is possible to enable mobile terminals to join the GSM systems. The integration of GSM, WLAN, and WiMAX bands will be one of the future trends for USB Dongles. Using the characteristics of monopole antennas, this study designs a basic monopole antenna (known as a reference antenna) and sets the operating frequency to a low center frequency of 1825 MHz and a high center frequency of WiMAX 3.3 GHz. Under the premise that no significant change occurs with the reference antenna structure, this paper proposes a dual-band design that is planar, simply designed, compact in size, independently matching, and with tunable frequencies that can cover the GSM1800 and WLAN bands to achieve the high tuning ratio of 1.6.

2. DUAL-BAND ANTENNA DESIGN

2.1. Antenna Structure

The proposed dual-band antenna structure for use in a GSM/WiMAX system is shown in Fig. 1. The antenna design is fabricated on an FR4 microwave substrate ($\varepsilon_r = 4.4$) with an area of $25 \times 20\,\text{mm}^2$ and a thickness of 1.6 mm equally divided into a ground plane section and a radiator section.

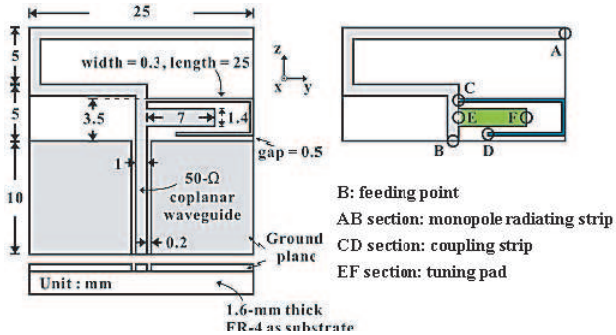

Figure 1. Dual-band antenna structure.

Antenna radiators as shown in Fig. 1 are mainly divided into three sections. The first section is the main radiator of the proposed dual-band antenna. The AB section (monopole radiator) is a radiator structure that extends from Point B (feeding point) as the starting point. The second section is the low frequency matching mechanism for the dual-band antenna.The CD section (coupling strip) isa coupling strip with a width of 0.3 mm and a total length of 25 mm that extends from the right edge of the AB radiator at a distance of 3.5 mm from the ground plane. The third section is the high frequency matching mechanism of the dual-band antenna. The EF section (tuning pad) extends from the right edge of the same AB structure body for a length of 7 mm and a width of 1.4 mm, and gap spacing of 0.5 mm between top and bottom of the coupling strip (CD section). The detailed structure and precise dimensions are shown in Fig. 1.

2.2. Monopole Antenna Design

To avoid over-coupling of the monopole radiation strip with the ground plane, the feed line is designed to extend from Point B (feeding point) to the half way point of the radiator (5 mm) before it is bent. This extends the monopole radiator to 45 mm, allowing it to meet the approximate 41 mm electric current path requirement ($^1/_4$ wavelength resonance) at a low frequency of 1.83 GHz. The antenna structure of such a design is shown in Fig. 2. This structure is called a reference antenna, and is used as the baseline for antenna design. As shown in the antenna simulation results in Fig. 3(a), this simple antenna structure can produce resonance at a low frequency mode of 1.825 GHz and a high frequency mode of 3.22 GHz. Moreover, it is noteworthy that the main reason for poor matching of the low frequency band in Fig. 3(a) is due to an antenna ground plane area that is relatively

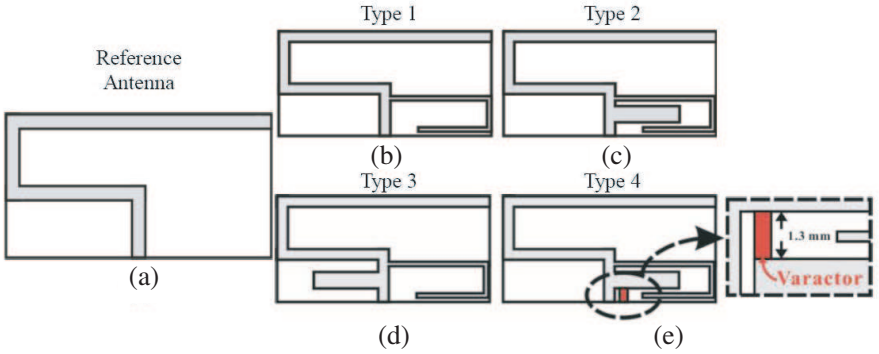

Figure 2. The development of the antenna design: (a) Reference antenna; (b) Type 1; (c) Type 2; (d) Type 3; (e) Type 4.

too small. The variations in ground plane significantly affect input impedance [13]. For unbalanced antennas, such as monopole antenna, the induced currents flowing on the ground plane also have a significant effect on the antenna performance. A minor current contribution may be incurred on the small, finite ground plane to radiate. Therefore, the input impedance becomes poor matched. The iterative adjustment of the ground size is not preferred to achieve the dual-band matching. Instead, we intended to design an independent and tunable dual-band matching mechanism suitable for the existing small ground plane area of a basic monopole antenna. The design produced Types 1 $\sim$ 4 antennas, which are separately described below.

2.3. Low Frequency Impedance Matching

As obtained from observation of the low frequency segment between 1.75 GHz $\sim$ 2 GHz of the Smith chart shown in Fig. 3(b), the impedance distribution curve of the reference antenna fell on the upper part of the Smith chart, indicating a lack of strong coupling. Under an effectively designed reference antenna structure without any significant alteration, a coupling strip (CD section) was modified and extended from the right edge of the antenna feed line. The coupling gap between the coupling strip and the ground plane was an adequately adjusted 0.5 mm. This structure is called a Type 1 antenna, as is shown in Fig. 2(b). Fig. 3(b) shows an increase in the amount of coupling for the coupling strip, which allows the imaginary part of the original impedance distribution curve to reduce, and a resonance ring occurs. This coupling stripforced the impedance of the low frequency to draw into the circle at VSWR = 2, achieving impedance matching.

In addition, as shown in Fig. 3(a), the low frequency of Type 1 at 1.825 GHz can generate a reflection loss of approximately −21.01 dB.

2.4. High Frequency Impedance Matching

Figure 3(a) shows deteriorating impedance at the high frequency section of the Type 1 antenna after connecting to a coupling strip because this antenna structure is of a single path type with dual-resonance. It is desired that high frequency matching can be similarly designed independently. With the use of antennas possessing enhanced inductiveness with impedance at a high frequency of 3.3 GHz, we

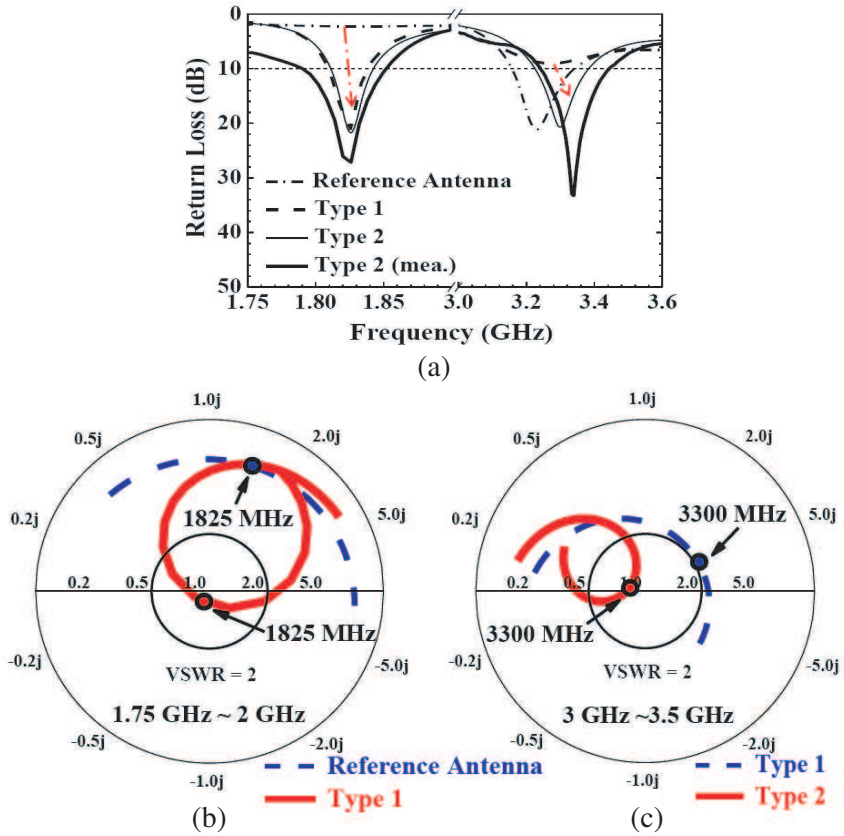

Figure 3. (a) The simulation of the antenna development from reference antenna to Type 1 and Type 2 antennas; (b) Smith chart for the low frequency matching; (c) Smith chart for the high frequency matching.

could design an effectively tuned tuning pad extending between the upper and lower spacing of the coupling strip. This structure is referred to as a Type 2 antenna (as shown in Fig. 2(c)). As shown in Fig. 3(c), the tuning pad can compensate for the high inductiveness at a high frequency of 3.3 GHz, allowing 3.3 GHz to achieve impedance matching while falling into the center of the Smith chart. As shown in Fig. 3(a), the data from actual and simulated Type 2 antennas are extremely close, which can already achieve impedance bandwidth of 1796 $\sim$ 1850 MHz at low frequency band and 3243 $\sim$ 3441 MHz at high frequency band. This novel type of low/high frequency matching mechanism is highly suitable for use in practical, basic monopole antenna designs.

2.5. Measurements Setup

HFSS EM software was applied to design and simulate the proposed antenna structure, and the designed antenna was fabricated by a milling machine. After that, Agilent E5071C Network Analyzer was used to measure the S parameter of the proposed antenna. To measure the far field performance, the fabricated antenna was delivered to a professional 3D anechoic chamber in Yageo Corporation (in Nantze Branch, Taiwan).

3. CURRENT DISTRIBUTION

Figure 4(a) shows the electric current distribution of a low frequency at 1.825 GHz. The terminating point of the electric current falls on the end of the monopole radiating strip. Because the low frequency mode is based on a $\frac{1}{4}$ wavelength resonance design, the maximal amplitude occurs at the beginning of the electric current, which gradually decays to a minimum towards the end of the electric current.

The electric current distribution diagram of a 3.3 GHz high-frequency is shown in Fig. 4(b). The maximal amplitude of the electric current appeared at approximately the half way point of the electric current path while the minimal amplitude appeared at the starting and terminating points. This electric current is designed at that time with a $\frac{1}{2}$ wavelength resonance mode.

It should be noted that the coupling strips in Figs. 4(a) and (b) have a comparatively strong electric current. The evidence of this is obtained from the fact that the high frequency matching of the Type 1 antenna in Fig. 3(a) deteriorated faster than did the reference antenna as a result of connecting to a coupling strip. The tuning pad, meanwhile, shows a comparatively strong electric current distribution

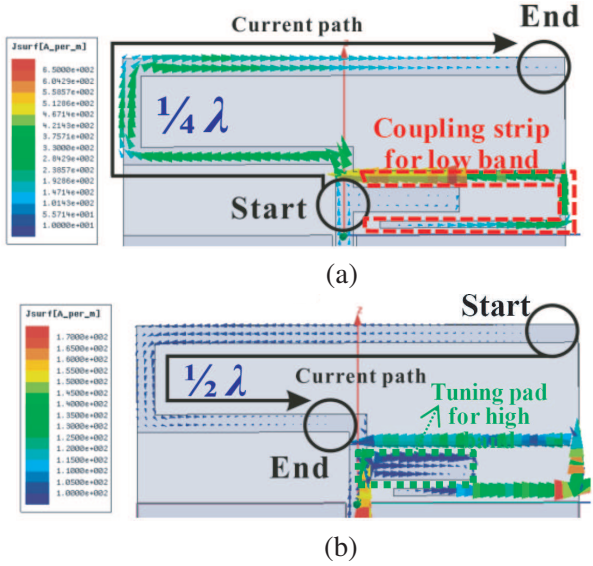

Figure 4. The current distribution at (a) 1.825 GHz; (b) 3.3 GHz.

only when operating at high frequency, as shown in Fig. 4(b). This also explains why the proposed antenna designs are based on low frequency matching as a priority.

4. CONTROL OF THE DUAL BANDS

The proposed antenna design could allow the monopole antenna to achieve both low and high frequency impedance matching. As shown in Fig. 6, the proposed tuning mechanism includes three major parameters, which set up a guideline for the development process of antenna design. To follow the development process of antenna design under various operating frequency conditions, the length L of the monopole radiator first had to be tuned to control the low operating frequency of the antenna, as shown in Fig. 5. The spacing w_s between the coupling strip (CD section in Fig. 1) and the edge of the substrate was then adjusted for low frequency impedance matching to facilitate the control of the amount of coupling between the coupling strip and the ground plane. Finally, the length d of the tuning pad was tuned to achieve high frequency impedance matching. By adjusting these three parameters (L, w_s, and d), the antenna can achieve dual-band performance.

By following the development process of antenna design, Type 2

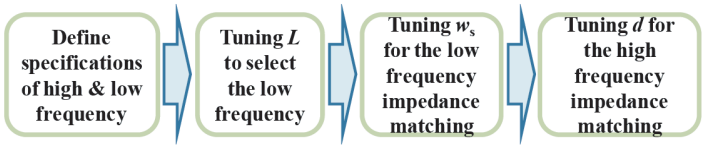

Figure 5. Flow chart of dual-band antenna design and tuning.

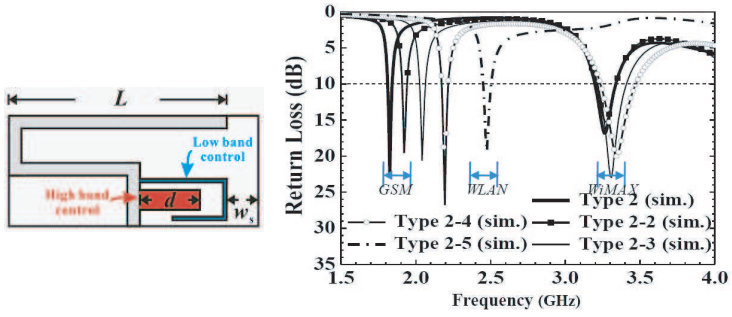

Figure 6. (a) The parameters of tuning the frequency bands and their corresponding controlling mechanism; (b) The simulation result of the antenna frequency tuning.

antenna is first used to discuss the performance of the proposed tuning mechanism as a compared baseline. Relevant antenna performance and parameter data are shown in Table 1. The tuning parts are as shown in Fig. 6(a). Fig. 6(b) showed the simulated performance diagram of the Type 2 series antenna, and the frequency tuning range can achieve 1.825 GHz $\sim$ 2.194 GHz, with a frequency ratio (largest f_L/smallest f_L) achieving 1.2. Type 2–5 antennas can also achieve impedance matching even though the low frequency was at 2.474 GHz. Since the coupling strip was already too close to the tuning pad, the tuning pad hadno optimized space. This led to the high frequency of Types 2–5 antennas being unable to achieve impedance matching. Relevant antenna performance and parameter data are shown in Table 1.

As mentioned previously, the coupling strip affects the available space of the tuning pad, so Types 2–5 antennas could not achieve impedance matching at the high frequency band. Moreover, the structure of coupling strip also limits the tuning ratio to 1.2. To improve the frequency tuning range, we proposed a modified design of the tuning pad structure, which separates the coupling strip and the tuning pad in different sides. This design is called Type 3 antennas

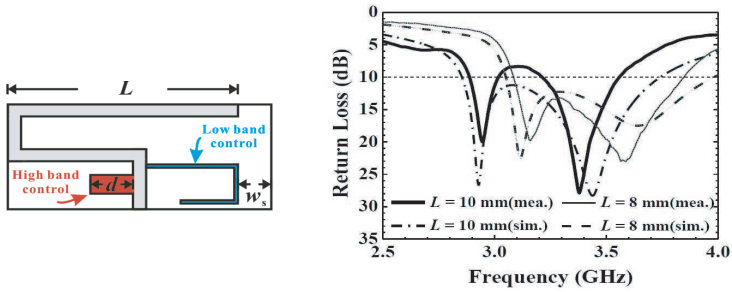

(a) (b)

Figure 7. (a) Antenna dual-band matching control mechanism; (b) Simulated and measured S_{11} diagram generated from various control parameters.

and shown in Fig. 2(d). This type of structure increases the selection space of low frequency parameter w_s and high frequency parameter d. The modified tuning diagram is shown in Fig. 7(a). By following the same antenna design process as mentioned previously (properly tuned L, w_s, and d according to the order mentioned previously), the low frequency tuning range can be directed to cover higher ranges. After optimizing the low frequency peak of Type 3 antenna to 2.943 GHz, the low frequency tuning range became 1.825 GHz $\sim$ 2.943 GHz, with a frequency ratio achieving 1.6. Therefore, the proposed control mechanism achieved a maximal tuning range with minimal area including the finite ground. Although the low frequency of Type 3–1 antenna could still be tuned to a higher frequency until it achieved 3157 MHz, if the strong coupling occurs at a high frequency, one broadband feature can be demonstrated. As a result, the high frequency mode was unable to maintain the characteristic of its original resonance mode. The relevant antenna performance parameter data are summarized in Table 1.

5. DESIGN WITH VARACTORS

In this paper, we also propose an alternative approach by using discrete components such as varactors, shown in Fig. 2(e). This design proves our analysis of tuning mechanism, but implements with a discrete component instead of coupled wires or pads. This structure, called Type 4, is primarily designed by adding a discrete capacitor placing between the pad and the ground plan. This design extends the ranges of the required coupling capacitance. In this paper, the original Types 2–5 (L = 10 mm) with high-frequency impedance matching

Table 1. The performance with different tuning parameters for the low bands.

Antenna Type (simulation)	L (mm)	w_s (mm)	d (mm)	The Central Lower Band (f_L) Frequency (MHz)	S_{11} (dB)
Type 2	25	0	7	1825	−22.8
Type 2–2	20	1	5.5	1921	−19.55
Type 2–3	17.5	2	5	2042	−20.6
Type 2–4	15	2.5	3	2194	−26.7
Type 2–5	10	5	4	2474	−19.3
Type 3	10	6	4	2943	−19.9
Type 3–1	8	7	3	3157	−19.8

cannot be reached due to the limitation of the gap between the pad and the wire. However, perfect matching can be feasibly fulfilled by arranging a discrete capacitor to improve impedance matching. It is worth mentioning that in this new design using the varactor, it is not necessary to modify any parameter of our antenna design in its geometry. This advantage not only avoids redoing antenna design, but also independently provides the tuning mechanism that we need. This design improves antenna impedance matching without inserting a matching network that may contribute to a certain amount of insertion loss. The performance of the antenna is shown in Fig. 8. From this figure, we also verify that the design pad is indeed equivalent to capacitive effects for antenna design.

6. INFLUENCE OF GROUND SIZES

Our proposed tuning mechanism also assists in shrinking the ground size. By shrinking the ground plane size, the overall antenna size, including the ground plane, will become practically compact. However, when the ground plane is too small, the antenna performance cannot be maintained. It has been studied that a small ground plane has a great effect on the antenna properties including input impedance and resonant frequency [13], so a finite ground plane consideration is necessary. From Fig. 9, the proposed matching mechanism is applied to achieve dual-band impedance matching when the antenna ground plane length increases to 20 mm and 30 mm. However, due to that changing

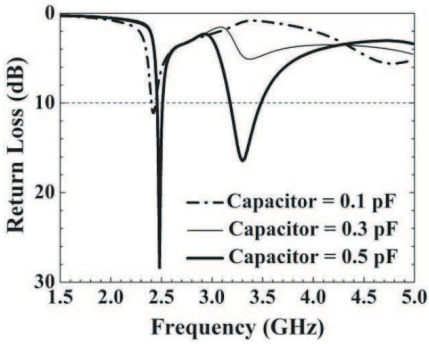

Figure 8. The simulated S_{11} of Type 4 antenna with variable capacitance values.

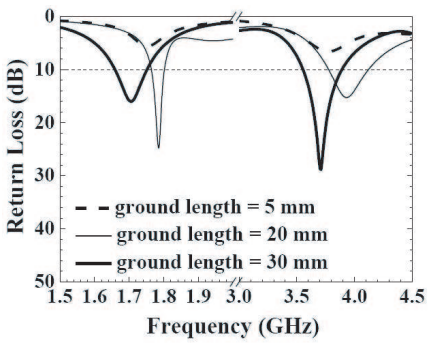

Figure 9. The simulation results of the ground size change (5, 20, and 30 mm) and a fixed width (25 mm) for the Type 2 antenna.

the ground area, the operation frequency of the antenna will cause the phenomenon of the frequency drift, which may be compensated by the proposed tuning mechanism. When the length of the ground plane reduces to below 5 mm, the proposed matching mechanism has been unable to reach matching any more. As long as the ground plane is relatively small with respect to the wavelength, a minor contribution of the ground plane currents is expected resulting in less radiation. Furthermore, the radiation resistance decreases as the ground length reduces [14], leading to a mismatching impedance. Therefore, the ground plane area of Type 2 antenna is the minimum area required for the dual band antenna design.

7. ANTENNA RADIATION PATTERN

Figures 10(a) and (b) show the 2D measured radiation pattern diagrams of Type 2 antenna at a low frequency of 1.83 GHz and a high frequency of 3.35 GHz, respectively. Figs. 11(a) and (b) show the 3D simulated radiation pattern diagrams of Type 2 antenna at a low frequency of 1.825 GHz and a high frequency of 3.3 GHz, respectively. As shown in these diagrams, low frequency mode antennas possess radiation patterns that are extremely close to omni-directional, quite consistent with what we expected from the appearance of omni-directional patterns in monopole antennas used in GSM mobile communication devices for various wireless environments. Fig. 12 shows the simulation data diagram of antenna gain and radiation efficiency of Type 2 antenna. The diagram shows that the antenna

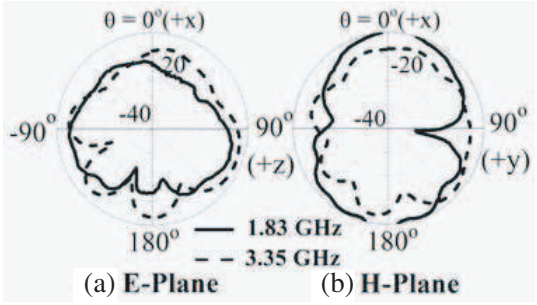

Figure 10. The measured 2D radiation patterns of the Type 2 antenna (a) Horizontal; (b) Vertical.

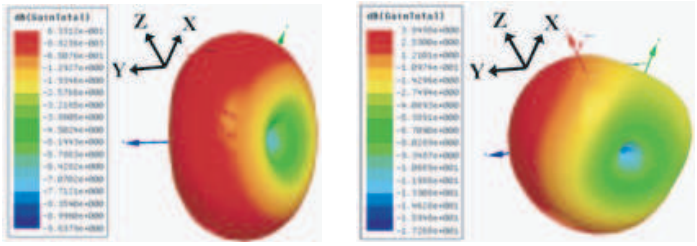

(a) (b)

Figure 11. The simulated 3D radiation pattern of the Type 2 antenna (a) 1.825 GHz; (b) 3.3 GHz.

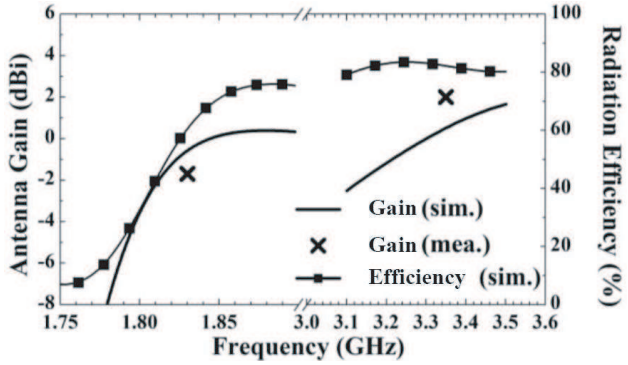

Figure 12. The simulated antenna gain and radiation efficiency of the Type 2 antenna.

radiation efficiency is about 60 to 80%, with a gain of approximately -0.3 to 1 dBi. The measured antenna gain is about -1.7 to 2 dBi.

8. CONCLUSION

This study proposes a dual-band antenna for the use in a GSM/WiMAX system with a total antenna size of $0.018\lambda_0^2$. A monopole antenna with a single path was used to generate resonance in dual-mode, thus achieving antenna size minimization. A matching technique was used to control this monopole antenna, allowing it to possess tunable dual band frequencies. The operating antenna was able to generate a low frequency ratio of 1.6 and maintain a favorable omni-directional radiation pattern for the use in GSM systems. The measured antenna gain was approximately $-1.7 \sim 2$ dBi, with a simulated radiation efficiency of $60 \sim 80\%$.

REFERENCES

1. Tsai, C.-L. and C.-L. Yang, "Highly efficient planar monopole antennas for 1.8/3.3 GHz dual band GSM/WiMAX operations," *IEEE Antennas and Propagation Society International Symposium* (*AP-S*), Jul. 2011.
2. *IEEE Standards Association (IEEE-SA) Standards*, Available: http://standards.ieee.org.
3. *The IEEE 802.16 Working Group on Broadband Wireless AccessStandards*, Available: http://wirelessman.org/.
4. Bialkowski, M. E., A. R. Razali, and A. Boldaji, "Design of an ultrawideband monopole antenna for portable radio transceiver," *IEEE Antenna Wireless Propag. Lett.*, Vol. 9, 554–557, 2010.
5. Lee, C. T. and K. L. Wong, "Uniplanar printed coupled-fed PIFA with a band-notching slit for WLAN/WiMAX operation in the laptop computer," *IEEE Trans. Antennas Propagat.*, Vol. 57, No. 4, 1252–1258, Apr. 2009.
6. Chaimool, S. and K. L. Chung, "CPW-fed mirrored-L monopole antenna with distinct triple bands for WiFi and WiMAX applications," *Electron. Lett.*, Vol. 45, No. 18, 928–929, Aug. 2009.
7. Chen, W. S. and Y. H. Yu, "Dual-band printed dipole antenna with parasitic element for WiMAX applications," *Electron. Lett.*, Vol. 44, No. 23, 1338–1339, Nov. 2008.
8. Shin, Y. S. and S. O. Park, "A compact loop type antenna for bluetooth, S-DMB, Wibro, WiMax, and WLAN applications," *IEEE Antenna Wireless Propag. Lett.*, Vol. 6, 320–323, 2007.

9. Kim, T. H. and D. C. Park, "CPW-fed compact monopole antenna for dual-band WLAN applications," *Electron. Lett.*, Vol. 6, 291–293, 2005.
10. Wong, K. L. and S. C. Chen, "Printed single-strip monopole using a chip inductor for penta-band WWAN operation in the mobile phone," *IEEE Trans. Antennas Propagat.*, Vol. 58, No. 3, 1011–1014, Mar. 2010.
11. Jeong, S. J. and K. C. Hwang, "Compact loop-coupled spiral antenna for multiband wireless USB dongles," *Electron. Lett.*, Vol. 46, No. 6, 388–390, Mar. 2008.
12. Lee, S. H. and Y. Sung, "Multiband antenna for wireless USB dongle applications," *IEEE Antenna Wireless Propag. Lett.*, Vol. 10, 25–28, 2011.
13. Zhang, Y., Z. N. Chen, and M. Y. W. Chia, "Characteristics of planar dipoles printed on finite-size PCBs in UWB radio systems," *IEEE Antennas and Propagation Society International Symposium* (*AP-S*), Jun. 2004.
14. Rmili, H., L. Aberbour, and C. Craeye, "On the radiation resistance of a planar monopole antenna with reduced ground plane," *IEEE Antenna Wireless Propag. Lett.*, Vol. 9, 732–736, 2010.